7-3-2013

Characterization of Freshwater Natural Dissolved Organic Matter (DOM): Mechanistic Explanations for Protective Effects Against Metaltoxicity and Direct Effects on Organisms

Hassan A. Al-Reasi
Wilfrid Laurier University, alreasi@squ.edu.om

Chris M. Wood
McMaster University

D. Scott Smith
Wilfrid Laurier University, ssmith@wlu.ca

Recommended Citation

Al-Reasi HA, Wood CM, Smith DS. Characterization of freshwater natural dissolved organic matter (DOM): Mechanistic explanations for protective effects against metal toxicity and direct effects on organisms. Environment International 2013;59:201-07.

Environment International 59 (2013) 201–207

Contents lists available at ScienceDirect

Environment International

journal homepage: www.elsevier.com/locate/envint

Characterization of freshwater natural dissolved organic matter (DOM): Mechanistic explanations for protective effects against metal toxicity and direct effects on organisms

Hassan A. Al-Reasi [a,b], Chris M. Wood [a], D. Scott Smith [b,*]

[a] Department of Biology, McMaster University, Hamilton, ON L8S 4K1, Canada
[b] Department of Chemistry, Wilfrid Laurier University, Waterloo, ON N2L 3C5, Canada

ARTICLE INFO

Article history:
Received 2 August 2012
Accepted 7 June 2013
Available online 3 July 2013

Keywords:
Natural organic matter
Metal speciation
Metal toxicity
Metal complexation
Biotic ligand model
Spectroscopy

ABSTRACT

Dissolved organic matter (DOM) exerts direct and indirect influences on aquatic organisms. In order to better understand how DOM causes these effects, potentiometric titration was carried out for a wide range of autochthonous and terrigenous freshwater DOM isolates. The isolates were previously characterized by absorbance and fluorescence spectroscopy. Proton binding constants (pK_a) were grouped into three classes: acidic ($pK_a \leq 5$), intermediate ($5 < pK_a \leq 8.5$) and basic ($pK_a > 8.5$). Generally, the proton site densities (L_T) showed maximum peaks at the acidic and basic ends around pK_a values of 3.5 and 10, respectively. More variably positioned peaks occurred in the intermediate pK_a range. The acid–base titrations revealed the dominance of carboxylic and phenolic ligands with a trend for more autochthonous sources to have higher total L_T. A summary parameter, referred to as the Proton Binding Index (PBI), was introduced to summarize chemical reactivity of DOMs based on the data of pK_a and L_T. Then, the already published spectroscopic data were explored and the specific absorbance coefficient at 340 nm (i.e. SAC_{340}), an index of DOM aromaticity, was found to exhibit a strong correlation with PBI. Thus, the tendencies observed in the literature that darker organic matter is more protective against metal toxicity and more effective in altering physiological processes in aquatic organisms can now be rationalized on a basis of chemical reactivity to protons.

1. Introduction

In freshwater environments, many abiotic and biotic processes are affected by water chemistry including natural organic matter (NOM). Aquatic NOM is a ubiquitous, naturally-occurring, heterogeneous mixture of organic compounds formed from the degradation of lignin-rich plant materials and the decay of dead organic biomass (Thurman, 1985). Based on filtration, the NOM fraction passing through a 0.45-μm membrane is known as dissolved organic matter (DOM) of which ≥50% by mass is carbon (Thurman, 1985). The concentration of DOM is widely variable in freshwater and commonly reported in mg C L^{-1} as dissolved organic carbon (DOC) (Thurman, 1985). The major chemical components (~50–90%) of DOM are humic substances which are operationally divided into humic and fulvic acids (MacCarthy, 1989; Thurman, 1985). In addition, carbohydrates, proteins, and amino acids make up lower proportions of most DOM samples (Thurman, 1985). DOM of allochthonous or terrigenous origin is composed mainly of humic substances, while that of autochthonous source (synthesized by biological activity within the water column) is made of humic substances with higher percentages of proteinaceous materials (McKnight et al., 2001). The heterogeneous nature of aquatic DOM is also reflected in the presence of diverse functional ligands expressing a wide range of acidity constants (pK_a) (Ritchie and Perdue, 2003; Smith and Kramer, 1999; Thurman, 1985).

As a global regulator in freshwater ecosystems, DOM has been investigated intensively for several indirect actions on organisms; these abiotic functions including attenuation of solar radiation, influences on carbon cycling and nutrient availability, and alteration of contaminant toxicity (Williamson et al., 1999). For example, protection against copper toxicity in the presence of aquatic DOM was correlated to the aromatic carbon content of DOM, estimated as specific absorbance at 254 or 340 nm (Al-Reasi et al., 2012; De Schamphelaere et al., 2004; Schwartz et al., 2004). In addition, humic fractions of 9 Norwegian DOMs showed strong correlation with the protective effect against copper toxicity (Ryan et al., 2004). Most recently, several absorbance and fluorescence characteristics were reviewed as quality indices of aquatic DOMs, and found to account for considerable variability in the protective effects against metal toxicity (Al-Reasi et al., 2011). Many direct interactions of DOM with aquatic organisms have also been demonstrated. For example, DOM molecules may accumulate on biological surfaces, influence membrane permeability, affect basic physiological functions, and induce toxic actions (Campbell et al., 1997; Galvez et al., 2009; Glover et al., 2005; Matsuo et al., 2006;

* Corresponding author. Tel.: +1 519 884 0710x3046.
E-mail address: ssmith@wlu.ca (D.S. Smith).

0160-4120/$ – see front matter © 2013 Elsevier Ltd. All rights reserved.
http://dx.doi.org/10.1016/j.envint.2013.06.005

Meinelt et al., 2007; Vigneault et al., 2002; Wood et al., 2003). These responses are widely variable, again possibly reflecting different DOM qualities.

Addressing the issue of DOM quality is a key step to understand how these ubiquitous substances act both directly and indirectly on organisms. Spectroscopic measurements have been successfully employed to tackle the quality of freshwater DOMs (Chen et al., 2002; Senesi et al., 1991). The UV–visible absorption properties have been utilized to detect the presence of chromophores (i.e. light absorbing moieties) of the heterogeneous DOMs. Despite the fact that the absorption spectra of DOMs are usually featureless, several measures have been proposed at specific wavelengths to approximate aromaticity (specific absorbance coefficient at 340 nm, SAC_{340}, Curtis and Schindler, 1997), the intensity of UV-absorbing absorbance groups to yellow-brown ones (absorbance ratios of 254 to 436 nm, $Abs_{254/436}$, Abbt-Braun and Frimmel, 1999), molecular weights (absorbance ratios of 254 to 365 nm, $Abs_{254/365}$, Dahlén et al., 1999) and octanol solubility ($Abs\text{-}octanol_{254}/Abs\text{-}water_{254}$, Gjessing et al., 1999). Similarly, fluorescence spectroscopy provides useful measures such as fluorescence index (FI = the ratio of the emission intensity at a wavelength of 450 nm to that at 500 nm, both obtained at an excitation wavelength of 370 nm) which can distinguish source or origin of various DOMs (McKnight et al., 2001). It also offers detailed qualitative molecular information about the major fluorophores of DOMs (i.e. light emitting moieties). For instance, excitation–emission matrices (EEMs) comprise simultaneous collections of numerous emission wavelengths over a range of excitation wavelengths (DePalma et al., 2011; McKnight et al., 2001). The EEMs can be depicted as three dimensional counter plots and as a result, the fluorophores or fluorescent components can be visualized as a function of excitation–emission pairs of wavelengths. Recent advances in handling of the EEMs by parallel factor analysis (PARAFAC) have improved identification of the components, and estimation of their abundance and the contribution of each one to the total fluorescence (Ishii and Boyer, 2012; Stedmon and Bro, 2008).

The long term objective of our research is to find simple-to-measure quality parameters to facilitate source-dependence corrections to DOC inputs for metal bioavailability and toxicity modeling, and to predict direct physiological effects on organisms. To this end, acid–base titrations have been utilized as an integrated measure of overall chemical reactivity for the DOM isolates. Then, the already published spectroscopic data for the same organic matters studied (Al-Reasi et al., 2012) have been discussed thoroughly and explored for the association with titration parameters.

2. Materials and methods

2.1. Collection, absorbance and fluorescence measurements of DOMs

The sampling was described in Al-Reasi et al. (2012). In brief, terrigenous and autochthonous DOM samples were collected by a portable reverse-osmosis unit from various natural freshwater bodies ranging widely in color and DOC concentrations (the clear water of Lake Ontario with ambient DOC of only 2 mg C L^{-1} to the brownish water of Luther Marsh of approximately 50 mg C L^{-1}). In addition, two commercially available humic substances, namely Aldrich humic acid (AHA, Sigma-Aldrich Chemical, St. Louis, MO, USA) and Nordic Reservoir NOM (NR, International Humic Substances Society, St. Paul, MN, USA) were included in chemical characterization. Most of the absorbance and fluorescence measurements of the different DOM sources have been detailed elsewhere (Al-Reasi et al., 2012). In the current study, normalized absorptions at the ultraviolet wavelength of 254 nm ($SUVA_{254} = Abs_{254}/DOC$) and at 436 nm ($SCOA_{436} = Abs_{436}/DOC$) were determined to estimate the presence of UV-absorbing and colored moieties of the samples, respectively (Abbt-Braun and Frimmel, 1999).

The fluorescence index (FI) was used as an indicator of DOM origin (McKnight et al., 2001) to evaluate its ability to distinguish sources of our samples. For fluorescence scans, EEMs of the DOMs were obtained after re-zeroing the fluorescence spectrophotometer (i.e. subtracting EEMs of the blank, ultrapure water) to minimize the influence of Raman scattering. The absorbance at 254 nm of the terrigenous isolates exceeded 0.3 absorbance units and therefore the EEMs of these samples were corrected using the absorbance in 200–600 nm as suggested by Ohno (2002) as follows:

$$I_0 = I \times 10^{(Abs_{ex}+Abs_{em})/2}$$

where I_0 is the corrected fluorescence intensity (i.e. in absence of self-absorption), I is the detected fluorescence intensity and Abs_{ex} and Abs_{em} are the absorbences at excitation and emission wavelengths, respectively. For each sample, the three-dimensional EEMs were processed to remove Rayleigh scattering, and then the processed EEMs were utilized to construct contour plots, a detailed fingerprint of the fluorescent components of each DOM source.

For PARAFAC analysis, the spectral EEMs were modeled using the PLS Toolbox from Eigenvector Research Inc. (Wenatchee, WA, USA) as implemented on the Matlab™ platform (The Mathworks Inc., Natick, MA, USA) as described elsewhere (Al-Reasi et al., 2012; DePalma et al., 2011). The PARAFAC modeling was carried out based on an *a priori* assumption of the presence of four fluorophores or components contained in the underlying fluorescence signal. Mathematically, the choice of the right number of the components to describe the fluorescence signal is difficult but it should be sufficient to describe the variation within the data set (Stedmon and Bro, 2008). In the present study, the selection of the four components was justified according to the fact that humic substances of aquatic DOMs are operationally defined into two fractions: fulvic and humic acids (Thurman, 1985), representing the two humic materials to be resolved by PARAFAC as humic-like and fulvic-like fluorophores. The heterogeneous DOM molecules can be separated into two chromatographic peaks; one with smaller molecular sizes and shorter fluorescence wavelengths (i.e. fulvic acids) and the other with bigger molecular sizes and longer fluorescence wavelengths (i.e. humic acids) (Wu et al., 2003, 2007). The other two fluorophores were proteinaceous materials and labeled as tryptophan-like and tyrosine-like. The model decomposed and quantified the underlying fluorophores mathematically (93.9% of the variability was explained and residual analysis showed no systematic trends), resulting in scores that were relative estimates of the abundances for each DOM sample.

2.2. Potentiometric acid–base titrations

Acid–base titrations were performed on diluted solutions (30 mg C L^{-1} of BL, PE, NR, LM and AHA) and the concentrated DOM isolates of LO and DC (Table 1). Eight to 16 titration replicates were carried out for each DOM sample. The ionic strength of each DOM solution was adjusted to 0.01 M with addition of 5 M potassium nitrate (KNO_3, Sigma Aldrich) and then the sample was transferred to the titration vessel. The sample was initially acidified with concentrated hydrochloric acid (HCl, Sigma Aldrich) to bring the pH down to ~2.0 and titrated at ~0.1 pH intervals by addition of 0.1 N sodium hydroxide (NaOH, made from standardized 1.005 N NaOH, Sigma Aldrich) to pH 12. At room temperature, all titrations were conducted in a CO_2-free atmosphere (i.e. under purge of ultrapure N_2 gas) using an automated titrator (848 Titrino Plus attached to 801 magnetic stirrer with support rod, Metrohm Canada) with a pH electrode (Orion 8101BNWP ROSS Half-Cell Electrode, Thermo Scientific) and a double junction Ag/AgCl reference electrode (Orion 900200 Sure-Flow Reference Half Cell Electrode, Thermo Scientific). To estimate proton binding constants (pK_a) and their site densities (L_T, μmol mg^{-1}), the experimental titration data were fitted to a fully optimized continuous

Table 1
Spectroscopic indices of aromatic composition (SAC_{340}), UV-absorbing molecules ($SUVA_{254}$) and yellow-brown colored moieties ($SCOA_{436}$)[a]. Data (mean ± standard errors of $n = 3$).

DOM source[b]	Code	SAC_{340}	$SUVA_{254}$	$SCOA_{436}$
Dechlorinated Hamilton water	DC	3.72 ± 0.07	1.51 ± 0.01	0.01 ± 0.00
Lake Ontario	LO	4.85 ± 0.10	1.40 ± 0.01	0.05 ± 0.00
Bannister Lake	BL	14.16 ± 0.07	2.49 ± 0.01	0.12 ± 0.00
Preston Effluent	PE	14.77 ± 0.30	2.32 ± 0.03	0.16 ± 0.01
Nordic Reservoir	NR	28.76 ± 0.52	3.78 ± 0.07	0.28 ± 0.01
Luther Marsh	LM	39.30 ± 0.37	4.42 ± 0.04	0.39 ± 0.00
Aldrich humic acid	AHA	79.98 ± 0.96	6.78 ± 0.08	1.34 ± 0.02

[a] SAC_{340}, $SUVA_{254}$ and $SCOA_{436}$ are the absorbances at 340 nm, 254 and 436 nm, respectively divided by DOC concentrations. See Al-Reasi et al. (2012) for other spectroscopic quality indices on these same samples.
[b] Sorted based on increasing color intensity according to SAC_{340}.

(FOCUS) model using in-house Matlab™ programs as described by Smith and Ferris (2001). Binding site densities within a specified pK_a range were determined by integration of the area under the curve in the pK_a spectrum.

2.3. Statistical analysis

Data have been presented as means ± 1 SEM (n) throughout. Normal distribution of the data for each quality measure was checked by Kolmogorov–Smirnov test. If not normally distributed, they were $\log_{10}$ transformed. The correlation between different DOM quality measures was then performed by the Pearson product moment correlation coefficient using SigmaStat for Windows (Version 3.5, Systat Software, Inc., Point Richmond, CA, USA). Significant correlation was established when $p < 0.05$.

3. Results and discussion

3.1. Absorbance and fluorescence indices

Absorbance and fluorescence indices have been summarized in Al-Reasi et al. (2012). Data assessing the aromatic composition (SAC_{340}) and the presence of the UV-absorbing molecules ($SUVA_{254}$) and yellow-brown colored moieties ($SCOA_{436}$) are presented in Table 1. The wide range of the aromaticity indices ($SUVA_{254}$ and SAC_{340}) indicated highly variable aromatic content of organic matter of the samples. Autochthonous DOMs (LO and BL) and PE (from a sewage treatment plant) had lower SAC_{340} values than those of terrigenous DOMs (NR and LM) and AHA. Usually, the terrigenous organic matter is composed of higher amount of aromatic carbon and phenols than the microbially derived or autochthonous DOMs and that is why the former is optically darker than the latter. Both the $SUVA_{254}$ and $SCOA_{436}$ increased from the colorless DC and LO to golden-brown AHA (Table 1). The ratio ($Abs_{254/436}$) provided an approximation of the abundance of UV-absorbing functional groups to the colored ones (Abbt-Braun and Frimmel, 1999). The $SUVA_{254}$ has been frequently employed to estimate aromatic content of organic compounds because the absorbance of energy at 254 nm corresponds to π–π* transitions typical of aromatic rings (Abbt-Braun and Frimmel, 1999). On the other hand, absorption of DOM in the visible range ($SCOA_{436}$) has been attributed to organic compounds with quinoide and ketoenol functional groups (Abbt-Braun and Frimmel, 1999). SAC_{340}, $SUVA_{254}$, and $SCOA_{436}$ emphasized the higher aromatic colored organic entities for the terrestrially derived DOMs compared to autochthonous DOMs. These quality indices were strongly correlated with one another ($r =$ 0.87–0.99), implying the consistency among all these measures to reflect the presence of aromatic and colored moieties in organic matter.

As indirect estimates of molecular weight, relatively higher values of $Abs_{254/365}$ were recorded for the autochthonous DOMs (LO, BL) and PE and lower values for the terrigenous ones (NR, LM) and AHA (Al-Reasi et al., 2012). Previous studies have demonstrated that the ratio increases as the average molecular weight of DOMs decreases (Chin et al., 1994; Dahlén et al., 1999). Therefore, $Abs_{254/365}$ may rank the examined DOMs in this decreasing order of average molecular weights, AHA > LM > NR > PE > BL > LO > DC. While this approach utilized absorbance ratio at 254 nm to that at 365 to indirectly look into molecular weights, determination of actual molecular weights of such complex molecules has been challenging given their ill-defined molecular structures and existence of countless isomers. Fattahi and Solouki (2003) calculated an average molecular weight of a Suwannee River fulvic acid sample using chemical equilibrium of aqueous solutions. While this cannot be validated for DOM isolates, this method resulted in a good agreement between the experimentally-calculated and actual molecular weights for chemicals with known molecular weights and structure (Fattahi and Solouki, 2003). This index ($Abs_{254/365}$) and that of the yellow-brown colored moieties ($SCOA_{436}$) were negatively correlated ($r = -0.97$), suggesting that smaller DOM molecules (i.e. higher values of $Abs_{254/365}$) may not contribute substantially to the light absorbance by the isolates, particularly autochthonous sources.

The UV–vis absorbance-based octanol solubilities ($Abs\text{-}octanol_{254}$/$Abs\text{-}water_{254}$) of our DOMs have been published elsewhere (Al-Reasi et al., 2012). This approach was earlier employed to approximate the liphophilic nature of aquatic DOM samples from the Norwegian Lakes (Gjessing et al., 1999). With exception of BL, DOMs of those considered autochthonous (i.e. DC, LO and PE) had higher octanol solubility than the terrigenous ones (LM, NR) and AHA (Al-Reasi et al., 2012). The positive correlation between this physicochemical property and the molecular weight index ($r = 0.78$) may imply that the smaller DOM molecules are more octanol soluble (i.e. more lipophilic). The liphophilic nature index was not related to aromatic carbon composition (SAC_{340} and $SUVA_{254}$) or to the presence of colored moieties of DOM ($SCOA_{436}$). Thus, aromatic and colored DOM molecules may not partition into the octanol phase. This is consistent with non-polar and colorless aliphatic carbon representing the types of moieties soluble in the octanol.

For natural sample UV/vis DOM quality parameters, it would be necessary to potentially take into account the influence of ferric iron on the light adsorption properties of chromphoric DOM (Xiao et al., 2013). For example at 340 nm a 5 mg C/L SRFA sample has an adsorption coefficient of 18 m^{-1} but that same SRFA 25% saturated with Fe(III) has an adsorption coefficient of almost 50 m^{-1}. For the current work, our samples were subjected to cation exchange though (Al-Reasi et al., 2012) so most of the Fe(III) should have been removed prior to our spectral characterizations.

According to source classification based on FI (McKnight et al., 2001), values of 2.5 and 1.9 for LO and PE respectively labeled their organic matter as autochthonous (Al-Reasi et al., 2012). On the other hand, NR and LM exhibited FI values of 1.2, indicating that organic matter in these freshwater sources is exclusively terrestrially-derived (Al-Reasi et al., 2012). The organic matter of BL, when originally sampled, was thought to be autochthonous based on visual examination on site, but it turned out to be of mixed origins (i.e. autochthonous and terrigenous) with an FI value of 1.5. An anomaly to this classification (where FI of ~1.9 represents autochthonous origin and ~1.4 represents terrigenous origin, McKnight et al., 2001) was the commercial AHA with a much lower FI of 0.83. Although it has been extensively used as a DOM model, AHA is not a real aquatic DOM substitute (Malcolm and MacCarthy, 1986). Interestingly, DC had a lower FI (1.8) than LO (2.5), shifting towards a terrigenous nature. This is most likely explained by changes in the molecular and structural composition of DC due to partial removal of the original organic matter from the source (LO) by filtration and addition of new organic matter probably by leaching of the activated charcoal during dechlorination. This explanation may not exclude the inherited heterogeneity of DOM molecules. While the origin index (FI) was inversely correlated with the aromatic

composition of the isolates (SAC_{340}, $r = -0.81$, and $SUVA_{254}$, $r = -0.86$), it was positively associated with the octanol solubility index (Abs-octanol$_{254}$/Abs-water$_{254}$, $r = 0.84$). Consequently and in contrast to terrigenous isolates, autochthonous DOMs would have higher amounts of dissolved organic molecules characterized by smaller sizes and higher octanol solubility.

The excitation–emission spectral contour plots for the 4 fluorophores (humic-like, fulvic-like, tryptophan-like and tyrosine-like) and their concentrations (normalized to DOC) resolved by PARAFAC were earlier presented in Al-Reasi et al. (2012). Other studies have reported similar fluorophores with characteristic fluorescence wavelengths for DOMs in different natural waters (Baker, 2001; DePalma et al., 2011; Fellman et al., 2008; Ishii and Boyer, 2012; Stedmon and Bro, 2008). The abundance of humic-like and fulvic-like components varied widely among the different DOM isolates, likely reflecting variable sources of organic matter. The humic-like component was the dominant fluorescent component in LM, NR and AHA accounting for >80% of their underlying fluorescence signal. In LO, BL and PE, between 16 and 50% of the fluorescence was accounted for as humic-like fluorophore (Al-Reasi et al., 2012). On the contrary, the abundance of the fulvic-like component was more prominent than humic-like for the autochthonous isolates (LO and PE) and DC (Al-Reasi et al., 2012). It is reasonable that more autochthonous sources include a greater proportion of lower molecular weight macromolecules. The contribution of tryptophan- and tyrosine-like fluorophores to the total fluorescence was much lower than that of the humic- and fulvic-like ones. In terrigenous isolates (LM and NR) and AHA, the fluorescence of proteinaceous materials was either negligible (tryptophan-like accounted for <5% of the total fluorescence) or completely absent (tyrosine-like fluorophore) (Al-Reasi et al., 2012). On the other hand, up to 20% of total fluorescence of DC, LO and BL were composed of tryptophan-like fluorophores, and there were variable contents of tyrosine-like fluorophores in autochthonous isolates (LO and PE), DC and PE (Al-Reasi et al., 2012).

Highly significant relationships were revealed for fluorescent components, in particular for the humic-like constituents. For example, the humic-like component appeared to govern the aromaticity of DOMs as this component was strongly and positively ($r \geq 0.90$) associated with SAC_{340}, $SUVA_{254}$ and $SCOA_{436}$. Opposite significant correlations were found between the fulvic-like fluorophore and SAC_{340} ($r = -0.78$), $SUVA_{254}$ ($r = -0.82$) and $SCOA_{436}$ ($r = -0.80$). Similarly, negative relationships were recorded for the humic-like component with octanol solubility index ($r = -0.84$), $Abs_{254/365}$ ($r = -0.89$) and FI ($r = -0.86$), implying that the molecules making up this fluorophore tend be of a less lipophilic nature with higher molecular sizes. Models suggest that DOM can exist as macromolecules either as random-coil shapes or aggregation of small molecules (Leenheer, 2007). In both cases, formation of macromolecules would mean keeping the lipophilic parts away from contact with water and consequently lower octanol solubility indices would be expected. No significant correlations were observed for the fulvic-like fluorophore with octanol solubility index, $Abs_{254/365}$ and FI. For protein-like materials, the tryptophan-like component did not show any significant association with the other spectroscopic quality measures. On the other hand, the tyrosine-like component was positively related to octanol solubility ($r = 0.90$) and FI ($r = 0.89$) and negatively correlated to humic-like fluorophore ($r = -0.81$). This is an indication of the tendency of the autochthonous DOMs to have a relatively higher proportion of protein-like substances.

3.2. Proton binding site densities and pK_a

The acid–base properties (acidity constants (pK_a) and their densities (L_T, μmol mg^{-1})) of the aquatic DOM samples are summarized in Fig. 1 as pK_a spectra, where site concentrations were assigned to each pK_a value in the range 2.6 to 11.2. The FOCUS method was based on the *a priori* assumption that the pK_a spectra will vary smoothly. Table 2 summarizes proton binding capacities in the range $pK_a \leq 5$ (acidic), $5 < pK_a \leq 8.5$ (intermediate) and $pK_a > 8.5$ (basic). In general, the proton affinity spectra showed peaks at the acidic end with pK_a maximum values around 3.5 and similar sized peaks at the basic end centered around a pK_a of 10. More variably positioned peaks occurred in the intermediate pK_a range. The most acidic peaks were generally interpreted as carboxylic sites, and the highest pK_a peaks as hydroxyl and more specifically phenolic sites (Smith and Kramer, 1999). The oxygen-containing functional groups, in particular the carboxylates and phenols, are the most abundant in DOM solutions (Chen et al., 2006; Dudal and Gerard, 2004; López et al., 2001). In fact, they are the most important in the determination of organic matter affinities for proton binding and metal complexation (Dudal and Gerard, 2004). In addition, metal binding occurs within the diffuse layer by means of electrostatic interactions due to effect of ionic strength of the solutions on charging behavior of DOM molecules (Dudal and Gerard, 2004; López et al., 2001). In the present study, the effect was ruled out since titrations of all isolates were conducted at constant ionic strength (0.01 M KNO_3). However, it should be noted that the titrations were carried out at DOC concentrations between 20 and 30 mg L^{-1}. López et al. (2001) performed titrations of fulvic acids at a concentration range of 25–90 mg L^{-1} and demonstrated that distribution of acid sites at each concentration may not be affected by the concentration of the electrolyte. Concerning optical properties of the same isolates (Al-Reasi

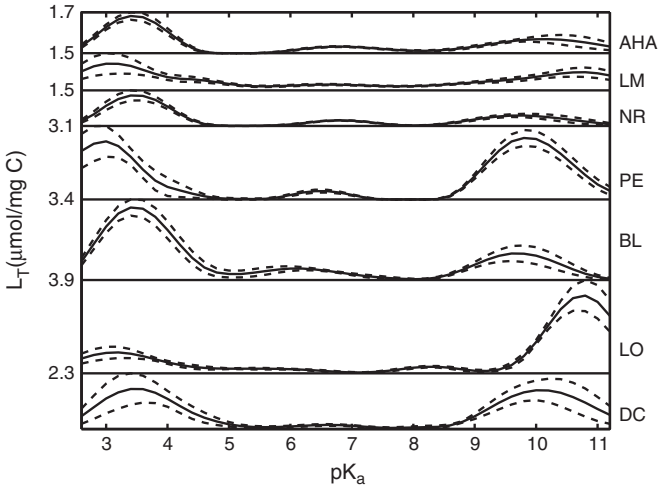

Fig. 1. pK_a spectra for each organic matter sample. The specific sample is indicated to the right of each plot. The y-axis labels for each solid line correspond to the maximum binding capacity of the pK_a spectrum below the line. Solid lines correspond to the mean spectrum (n in the range 5 to 15) and the dashed lines correspond to standard errors. The samples are stacked from highest SAC_{340} for the top spectra to the lowest SAC_{340} value at the bottom.

Table 2
Binding capacities for acidic sites ($pK_a < 5$), intermediate sites (pK_a 5 to 8.5) and basic sites ($pK_a > 8.5$) as determined by integration of the area under the curve within the specified pK_a value ranges. Bidentate capacity is determined as the average of acidic and basic site capacities. Proton Binding Index (PBI) is the ratio between intermediate pK_a and bidentate capacity. Data (mean ± standard errors for n observations).

Code	Binding capacities (L_T, μmol mg^{-1})				
	Acidic	Intermediate	Basic	PBI	n
DC	2.56 ± 0.99	0.36 ± 0.13	2.86 ± 0.96	0.13 ± 0.05	10
LO	1.32 ± 0.32	0.50 ± 0.09	3.75 ± 0.66	0.20 ± 0.04	10
BL	4.26 ± 0.68	0.89 ± 0.24	1.79 ± 0.55	0.30 ± 0.08	9
PE	2.67 ± 0.86	0.38 ± 0.09	4.08 ± 0.60	0.11 ± 0.03	8
NR	1.58 ± 0.27	0.31 ± 0.04	0.79 ± 0.20	0.26 ± 0.03	11
LM	1.74 ± 0.53	0.70 ± 0.08	1.45 ± 0.29	0.44 ± 0.05	16
AHA	1.89 ± 0.23	0.49 ± 0.05	1.17 ± 0.31	0.32 ± 0.04	10

et al., 2012), basic proton binding capacities (and $pK_a > 8.5$) demonstrated significant correlations with octanol solubility index ($r = 0.82$), FI ($r = 0.88$) and humic-like fluorophore ($r = 0.77$). The sum of binding capacities was significantly related to fulvic-like fluorophore ($r = 0.79$). All other relationships turned out to be insignificant.

Inspection of Fig. 1 illustrated that the darker organic matters tend towards less total capacity; the maximum L_T values tend towards smaller values as the SAC_{340} values increase. To better visualize the relationship between color and proton reactivity, a contour plot is presented in Fig. 2 with the scans presented in the same order as in Fig. 1. There seemed to be little trend in the acidic pK_a values, but overall the intensity decreased as the DOM became darker in color. The most basic peaks were more variable in location but with the same overall trend of decreasing intensity as the samples became darker in color. Based on $SAC_{340-350}$, overall darker organic matter has been observed to be more protective metal toxicity (e.g. Al-Reasi et al., 2012; De Schamphelaere et al., 2004; Ryan et al., 2004; Schwartz et al., 2004). Protons react at the same types of functional groups as metals; thus, at first appearance the decreased capacity with darker color appeared counterintuitive. However, carboxylic and phenolic sites are not strong metal binding centers in and of themselves, and capacity alone is not sufficient to predict potential impacts on metal bioavailability. For example, high capacity weak sites would not tend to be very protective if binding sites on the organism have higher affinity (log$K$). However, what determines the competition between complexation in solution and binding to the organism's surface is not the affinity constant alone (Log$K$), but rather the product ($L_T \times K$) (see preface in SETAC, 2009).

3.3. Relationship between spectroscopic properties and acidic functional group analysis

Several different approaches were tested to link chemical reactivity, as defined by proton pK_a and L_T, to optical properties. Individual acid, base and intermediate binding sites did not link to spectroscopy in any clear way, statistically or conceptually. Thus, a mathematical combination of proton binding sites is required to link reactivity and spectroscopy. The logic of the new proposed proton binding metric is as follows. In metal speciation modeling, tridentate sites represent very strong metal binding sites; monodentate sites tend to be weaker and exhibit binding at high loadings of metal (i.e., for Fe(III) in Xiao et al., 2013) whereas a tridentate site would be significant at low levels of total metal. The concept of strong tridentate binding is typified by the representation of the strongest binding sites as tridentate sites in the geochemical complexation model, Windermere Humic Aqueous Model (WHAM) (Tipping, 1998). There are three main proton binding classes of ligands identified here and a model tridentate ligand would have three pK_a values (for example, consider citric acid, phosphoric acid or diethylenetriamine). If these three sites are in 1:1:1 proportions, DOM could be represented as a single triprotic ligand. Similarly, DOM can form additional bonds with metal resulting in more stable tetradentate, pentadentate and hexadentate complexes (Chen et al., 2006) but if such strong sites exist they will occur at very low concentrations and in terms of metal binding would be saturated at levels of total metal where toxicity is observed in natural systems.

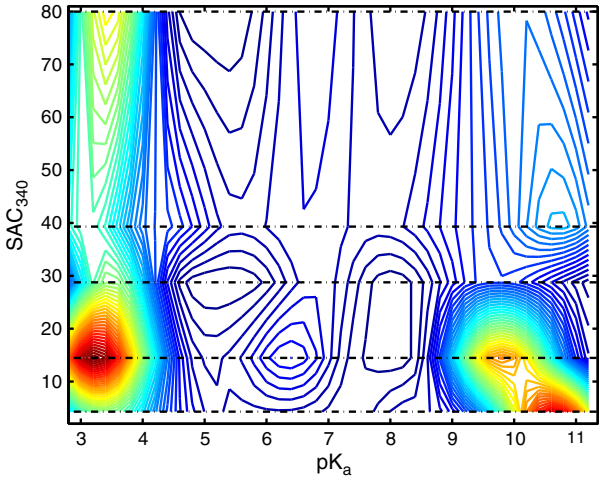

Fig. 2. Interpolated contour plot of the binding capacity (L_T) versus pK_a and SAC_{340}. The horizontal dashed lines correspond to each of 5 different SAC_{340} values where the values near 4 and 15 are the average of DC and LO, and BL and PE samples, respectively. Note: interpolated contour lines are intended to help with visualization of the data trends only. Measured values are only recorded as indicated by the horizontal lines.

Here a Proton Binding Index (PBI) is used to measure the difference between actual measurements and the model tridentate ligand hypothesis. To estimate the potential of the organic matters in this study to show strong tridentate binding, a PBI was calculated as:

$$PBI = \frac{\text{int}}{((acid + base)/2)}$$

where, *PBI* is a function of the measured *acid*, *base* and intermediate (*int*) proton binding capacities. The idea of this calculation was that the numerator represents the average capacity for bidentate complex formation (i.e. salicylic acid-like with a phenolic group ortho to a carboxylic group). The average value was selected because both acid and base sites have error associated with them and there is no way to know which would be stoichiometrically limiting. The third proton binding site that could be involved in a tridentate complex was represented by the sum of intermediate proton binding capacity. A value of PBI = 1 would correspond to a stoichiometric amount of intermediate proton binding sites to match the hypothetical bidentate site. In general PBI should be less than one and high values would represent stronger potential for binding. Results of PBI calculations are presented in Table 2 and plotted versus SAC_{340} in Fig. 3(a).

Overall, darker organic matter had a higher PBI value and is expected to be more protective against metal toxicity. The seven samples used in this study were plotted versus SAC_{340} (Fig. 3a), as well as DOM samples from the NOM-Typing project as titrated in Smith and Kramer (1999). The NOM-Typing samples were not used in determination of the regression line in Fig. 3 and without calibration these samples fall within the 95% confidence interval of the new data presented here. For comparison, the PBI value calculated from the data of Smith and Kramer (1999) for titration of Suwannee River Fulvic Acid has also been included. Thus, except for the "unnatural" AHA, all the samples considered follow the general trend of darker organic matter having higher PBI. This interpretation is consistent with the observation that darker organic matter is more protective (Al-Reasi et al., 2012; De Schamphelaere et al., 2004; Ryan et al., 2004; Schwartz et al., 2004). From a detailed consideration of acid–base titration data, it seems that darker organic matter has a greater potential to form strong binding with metals as demonstrated by the PBI calculation. The PBI calculation involves a large assumption; that three ionizable sites are involved in tridentate metal complexation. Nevertheless, it does produce excellent correlations with color and thus tendencies for metal reactivity.

To assess PBI as a potential toxicity indicator variable, Fig. 3(b) demonstrates a strong linear relationship ($r^2 = 0.779$, $p = 0.008$) between PBI and Cu LC_{50} for *Daphnia magna* in the same DOM samples. The LC_{50} values are taken from Al-Reasi et al. (2012). Interestingly, the Aldrich humic acid sample now falls on the trend line; thus, PBI may in fact be a better "quality indicator" than SAC_{340}. In Al-Reasi et al. (2012), AHA did not correlate with the linear SAC_{340} toxicity prediction relationship followed by the other samples. This is a reasonable possibility given that PBI is directly determined for each DOM by reactivity whereas SAC_{340} is not directly related to

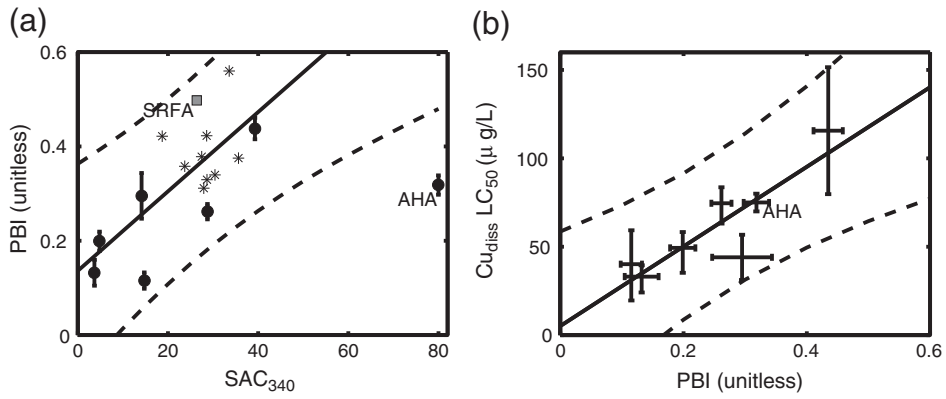

Fig. 3. (a) Proton Binding Index (PBI) versus SAC_{340} and (b) LC50 versus PBI. The error bars correspond to 95% confidence intervals about the measured data. Suwannee River Fulvic Acid (SRFA) and Aldrich Humic acid (AHA) are indicated by text adjacent to corresponding data points. ✳ symbols correspond to DOM samples from the NOM-Typing project (e.g. Abbt-Braun and Frimmel, 1999; Gjessing et al., 1999). LC_{50} values are taken from Al-Reasi et al., 2012. Dashed lines indicate 95% confidence interval about the solid regression lines.

reactivity. Aldrich humic acid is known to have high ash content, according to Chiou et al. (1987), the ash content of Aldrich humic acid may reach up to 31%. Any reactivity of this ash content will be reflected in the PBI but not for SAC_{340} which is related to aromatic groups in the DOM.

Addressing the quality issue of DOM is of environmental significance not just for the direct and indirect effects on aquatic organisms but also for other processes in natural waters. For example, simple optical properties of DOM can help to improve predictions of nitrate removal (Barnes et al., 2012) and can be employed to allocate the seasonal and spatial variations in the formation of the harmful disinfection byproducts associated with the chlorination of raw water (Herzsprung et al., 2012). In future, it will be of interest to evaluate the PBI approach in this regard.

The quality indices, explored above, provide easy-to-measure parameters obtained using simple absorbance, fluorescence, and titration measurements to probe molecular and structural chemistry of distinct aquatic DOM sources. These indices, as quality measures, will help researchers to evaluate the abiotic and biotic roles of DOM in the natural freshwaters. Concerning the protective effect against metal toxicity in particular, the spectroscopic parameters can be related to chemistry of metal binding through the PBI parameter. Our overall conclusion is that darker organic matter is more protective against metal toxicity, and more effective at interacting with physiological processes, because darker organic matter has a greater proton binding ratio as determined by PBI. The specific structural reasons for this correlation will require further investigation.

Acknowledgments

This work was supported by Discovery grants from the Natural Sciences and Engineering Research Council of Canada (NSERC) to CMW and DSS. CMW is supported by the Canada Research Chair Program. The authors wish to thank Prof. Peter Campbell and the two anonymous reviewers for their useful comments and suggestions on the original manuscript. Special appreciation goes to the Government of Oman for providing a doctoral scholarship for HAA.

References

Abbt-Braun G, Frimmel FH. Basic characterization of Norwegian NOM samples—similarities and differences. Environ Int 1999;25:161–80.
Al-Reasi HA, Smith DS, Wood CM. Evaluating the ameliorative effect of natural dissolved organic matter (DOM) quality on copper toxicity to *Daphnia magna*: improving the BLM. Ecotoxicology 2012;21:524–37.
Al-Reasi HA, Wood CM, Smith DS. Physicochemical and spectroscopic properties of natural organic matter (NOM) from various sources and implications for ameliorative effects on metal toxicity to aquatic biota. Aquat Toxicol 2011;103:179–90.
Baker A. Fluorescence excitation–emission matrix characterization of some sewage-impacted rivers. Environ Sci Technol 2001;35:948–53.
Barnes RT, Smoth RL, Aiken GR. Linkage between denitrification and dissolved organic matter quality, Boulder Creek watershed, Colorado. J Geophys Res 2012;117: G01014.
Campbell PGC, Twiss MR, Wilkinson KJ. Accumulation of natural organic matter on the surfaces of living cells: implications for the interaction of toxic solutes with aquatic biota. Can J Fish Aquat Sci 1997;54:2543–54.
Chen J, Gu B, LeBoeuf EJ, Pan H, Dai S. Spectroscopic characterization of the structural and functional properties of natural organic matter fractions. Chemosphere 2002;48:59–68.
Chen J, Gat P, Frimmel FH, Abbt-Braun G. Metal binding by humic substances and dissolved organic matter derived from compost. In: Twardowska I, Allen HE, Häggblom MM, editors. Soil and water pollution monitoring, protection and remediation. Springer; 2006. p. 3–23.
Chin YP, Aiken G, O'Loughlin E. Molecular weight, polydispersity, and spectroscopic properties of aquatic humic substances. Environ Sci Technol 1994;28:1853–8.
Chiou CT, Kile DE, Brinton TI, Malcolm RL, Leenheer JA, MacCarthy A. Comparison of water solubility enhancements of organic solutes by aquatic humic materials and commercial humic acids. Environ Sci Technol 1987;21:1231–4.
Curtis PJ, Schindler DW. Hydrologic control of dissolved organic matter in low-order Precambrian Shield Lakes. Biogeochemistry 1997;36:125–38.
Dahlén J, Bertilsson S, Pettersson C. Effects of UV-A irradiation on dissolved organic matter in humic surface waters. Environ Int 1999;22:501–6.
DePalma SGS, Arnold WR, McGeer JC, Dixon DG, Smith DS. Variability in dissolved organic matter fluorescence and reduced sulphur concentration in coastal marine and estuarine environments. Appl Geochem 2011;26:394–404.
De Schamphelaere KAC, Vasconcelos FM, Tack FMG, Allen HE, Janssen CR. Effect of dissolved organic matter source on acute copper toxicity to *Daphnia magna*. Environ Toxicol Chem 2004;23:1248–55.
Dudal Y, Gerard F. Accounting for natural organic matter in aqueous chemical equilibrium models: a review of the theories and applications. Earth Sci Rev 2004;66: 199–216.
Fattahi A, Solouki T. Using solution equilibria to determine average molecular weight of the Suwannee River fulvic acids. Anal Chim Acta 2003;496:325–37.
Fellman JB, D'Amore DV, Hood E, Boone RD. Fluorescence characteristics and biodegradability of dissolved organic matter in forest and wetland soils from coastal temperate watersheds in southeast Alaska. Biogeochemistry 2008;88:169–84.
Galvez F, Donini A, Playle RC, Smith S, O'Donnell M, Wood CM. A matter of potential concern: natural organic matter alters the electrical properties of fish gills. Environ Sci Technol 2009;42:9385–90.
Gjessing ET, Egeberg PK, Hikedal JT. Natural organic matter in drinking water—the "NOM-typing project", background and basic characterization of the original water samples and NOM isolates. Environ Int 1999;25:145–59.
Glover C, Pane EF, Wood CM. Humic substances influence sodium metabolism in the freshwater crustacean *Daphnia magna*. Physiol Biochem Zool 2005;78:405–16.
Herzsprung P, Tümpling WV, Hertkorn N, Harir M, Büttner O, Bravidor J, et al. Variations of DOM quality in inflows of a drinking water reservoir: linking of van Krevelen diagrams with EEMF Spectra by Rank Correlation. Environ Sci Technol 2012;46:5511–8.
Ishii SKL, Boyer TH. Behavior of reoccurring PARAFAC components in fluorescent dissolved organic matter in natural and engineered systems: a critical review. Environ Sci Technol 2012;46:2006–17.
Leenheer JA. Progression from model structures to molecular structures of natural organic matter components. Annals Environ Sci 2007;1:57–68.
López R, Fiol S, Antelo JM, Arce F. Effect of fulvic acid concentration on modeling electrostatic and heterogeneity effects in proton binding reactions. Anal Chim Acta 2001;434:105–12.
MacCarthy P. Bioavailability and toxicity of metals and hydrophobic organic contaminants. In: Suffet IH, MacCarthy P, editors. Aquatic humic substances: influence on fate and treatment of pollutants. Washington DC: American Chemical Society; 1989. p. 263–79.

Malcolm RL, MacCarthy P. Limitations in the use of commercial humic acids in water and soil research. Environ Sci Technol 1986;20:904–11.
Matsuo AYO, Woodin BR, Reddy CM, Val AL, Stegeman JJ. Humic substances and crude oil induce CYP1A expression in the Amazonian fish species *Colossoma macropomum* (tambaqui). Environ Sci Technol 2006;40:2851–8.
McKnight DM, Boyer EW, Westerhoff PK, Doran PT, Kulbe T, Andersen DT. Spectrofluorometric characterization of dissolved organic matter for indication of precursor organic material and aromaticity. Limnol Oceanogr 2001;46:38–48.
Meinelt T, Paul A, Phan TM, Zwirnmann E, Krüger A, Wienke A, et al. Reduction in the vegetative growth of the water mold *Saprolegnia parasitica* (Coker) by humic substances of different qualities. Aquat Toxicol 2007;83:93–103.
Ohno T. Fluorescence inner-filtering correction for determining the humification index of dissolved organic matter. Environ Sci Technol 2002;36:742–6.
Ritchie JD, Perdue EM. Proton-binding study of standard and reference fulvic acids, humic acids, and natural organic matter. Geochim Cosmochim Acta 2003;67:85–96.
Ryan AC, VanGenderen EJ, Tomasso JR, Klaine SJ. Influence of natural organic matter source on copper toxicity to larval fathead minnows (*Pimephales promelas*): implications for the biotic ligand model. Environ Toxicol Chem 2004;23:1567–74.
Schwartz ML, Curtis PJ, Playle RC. Influence of natural organic matter on acute copper, lead, and cadmium toxicity to rainbow trout (*Oncorhynchus mykiss*). Environ Toxicol Chem 2004;23:2889–99.
Senesi N, Miano TM, Provenzano MR, Brunetti G. Characterization, differentiation, and classification of humic substances by fluorescence spectroscopy. Soil Sci 1991;152:259–71.
SETAC. Copper: environmental fate, effects, transport and models: papers from environmental toxicology and chemistry, 1982 to 2008 and integrated environmental assessment and management, 2005 to 2008. In: Gorsuch JW, Arnold WR, Santore RC, Smith DS, Reiley MC, editors. DVD. Society of Environmental Toxicology and Chemistry; 2009.
Smith DS, Ferris FG. Proton binding by hydrous ferric oxide and aluminum oxide surfaces interpreted using fully optimized continuous pK_a spectra. Environ Sci Technol 2001;35:4637–42.
Smith DS, Kramer JR. Multi-site proton interactions with natural organic matter. Environ Int 1999;25:307–14.
Stedmon CA, Bro R. Characterizing dissolved organic matter fluorescence with parallel factor analysis: a tutorial. Limnol Oceanogr: Methods 2008;6:572–9.
Thurman EM. Geochemistry of Natural Waters. Dordrecht: Martinus Nijhof/DR W. Junk Publishers; 1985 [Kluwer Academic Publishers Group].
Tipping E. Humic ion-binding model VI: an improved description of the interactions of protons and metal ions with by humic substances. Aquat Geochem 1998;4:3–47.
Vigneault B, Percot A, Lafleur M, Campbell PGC. Permeability changes in model and phytoplankton membranes in the presence of aquatic humic substances. Environ Sci Technol 2002;34:3907–13.
Williamson CE, Morris DP, Pace ML, Olson OG. Dissolved organic carbon and nutrients as regulators of lake ecosystems: resurrection of a more integrated paradigm. Limnol Oceanogr 1999;44:795–803.
Wood CM, Matsuo AYO, Wilson RW, Gonzalez RJ, Patrick ML, Playle RC, et al. Protection by natural blackwater against disturbances in ion fluxes caused by low pH exposure in freshwater stingrays endemic to the Rio Negro. Physiol Biochem Zool 2003;76:12–27.
Wu FC, Evans RD, Dillon PJ. Separation and characterization of NOM by high-performance liquid chromatography and on-line three-dimensional excitation emission matrix fluorescence detection. Environ Sci Technol 2003;37:3687–93.
Wu FC, Evans RD, Dillon PJ, Cai YR. Rapid quantification of humic and fulvic acids by HPLC in natural waters. Appl Geochem 2007;22:1598–605.
Xiao Y-H, Sara-Aho T, Hartikainen H, Vähätalo AV. Contribution of ferric iron to light adsorption by chromophoric dissolved organic matter. Limnol Oceanogr 2013;58:653–62.